

Hint towards inconsistency between BAO and Supernovae Dataset: The Evidence of Redshift Evolving Dark Energy from DESI DR2 is Absent

Samsuzzaman Afroz , Suvodip Mukherjee 

Department of Astronomy and Astrophysics, Tata Institute of Fundamental Research, 1, Homi Bhabha Road, Mumbai 400005, India

E-mail: samsuzzaman.afroz@tifr.res.in, suvodip@tifr.res.in

Abstract. The combination of independent cosmological datasets is a route towards precision and accurate inference of the cosmological parameters if these observations are not contaminated by systematic effects. However, the presence of unknown systematics present in different datasets can lead to a biased inference of the cosmological parameters. In this work, we test the consistency of the two independent tracers of the low-redshift cosmic expansion, namely the supernovae dataset from Pantheon+ and the BAO dataset from DESI DR2 using the distance duality relation which is a cornerstone relation in cosmology under the framework of General Relativity. We find that these datasets violate the distance duality relation and show a signature of redshift evolution, hinting toward unaccounted physical effects or observational artifacts. Coincidentally this effect mimics a redshift evolving dark energy scenario when supernovae dataset and DESI datasets are combined without accounting for this inconsistency. Accounting for this effect in the likelihood refutes the previous claim of evidence of non-cosmological constant as dark energy model from DESI DR2, and shows a result consistent with cosmological constant with $w_0 = -0.92 \pm 0.08$ and $w_a = -0.49^{+0.33}_{-0.36}$. This indicates that the current conclusion from DESI DR2 in combination with Pantheon+ is likely due to the combination of two inconsistent datasets resulting in precise but inaccurate inference of cosmological parameters. In the future, tests of this kind for the consistency between different cosmological datasets will be essential for robust inference of cosmological parameters and for deciphering unaccounted physical effects or observational artifacts from supernovae and BAO datasets.

Contents

1	Introduction	1
2	A Primer on the CDDR Test	4
3	Data-Driven CDDR Test for supernovae samples and DESI DR2	4
4	Methodology for Joint Analysis of SNIa and BAO Data	6
4.1	Baseline Inference without the Distance Duality Coefficient in the likelihood	6
4.2	Extended Inference with a Distance Duality Coefficient	7
5	Results	9
5.1	Baseline case: No inclusion of distance-duality coefficient in the likelihood	9
5.2	Extended case: Inclusion of distance-duality coefficient in the likelihood	10
5.3	Summary of all the cases	10
6	Discussion on the scientific implication of our findings	11
7	Conclusion	13

1 Introduction

The combination of independent cosmological datasets has long been recognized as a pathway to both precise and accurate determination of fundamental cosmological parameters[1–6]. Independent measurements such as those from supernovae type Ia (SNIa), baryon acoustic oscillations (BAO), and the cosmic microwave background (CMB) have historically converged on a consistent model of the universe with dark matter and dark energy, apart from the disagreement in the value of the current expansion rate of the Universe (known as the Hubble constant) inferred from low redshift and high redshift probes [7–13].

The advent of DESI marks the beginning of a new era in high-precision BAO observations, as it measures the large-scale clustering of galaxies and quasars across an extensive redshift range[10, 14, 15]. The DESI DR2 results are combined with the low redshift luminosity distance measurement from SNIa from the Pantheon+[16], Union[17], and DESY5[18] datasets to improve the precision on the inference of the low redshift expansion history of the Universe and hence obtaining tighter constraints on the dark energy equation of state (EoS) using the Chevallier-Polarski-Linder (CPL) parameterization[19–21]. This data in combination with other cosmological probes denoted a strong evidence toward a evolving dark energy, and shows evidence towards ruling out cosmological constant with a statistical significance of 2.8 to 4.2 after including BAO measurements with CMB and supernovae [10]. These results deliver compressed distance observables that, after rigorous internal consistency checks of the line of sight and angular BAO measurements [22]. Though such parametrization is a simple step towards exploring the dark energy evolution, its connection with the theoretical models are often questioned [23–25] and more physics-driven models are essential to discover the dark energy EoS. However, a more crucial point to scrutinize to gauge the validity of this inference is the internal consistency of the different cosmological datasets used for deriving the dark energy EoS.

In this study, we use the consistency test based on the cosmic distance duality relation (CDDR), which is valid under the General Theory of Relativity for any expansion history of the Universe [26, 27]. The CDDR connects the luminosity distance and the angular-diameter distance, as expressed in Equation 2.1, as a function of cosmological redshift. Any two independent datasets of the cosmological distances say luminosity distance from supernovae and angular diameter distance from BAO, with the source redshifts inferred spectroscopically, should satisfy the CDDR. It is important to note that this relation holds for any dark energy EoS, according to the Etherington’s reciprocity theorem [28]. However, if there is an unknown physical or systematic effect present in the datasets, then violation from this relation is expected. As a result, CDDR can provide a physics-based consistency test between the datasets and any signature of disagreement of this consistency relation can hint towards a breakdown of at least one of the assumptions made in the analysis. We demonstrate this aspect on how the combining incorrect posteriors on the cosmological parameters can lead to a biased inference by a schematic diagram in Figure 1.

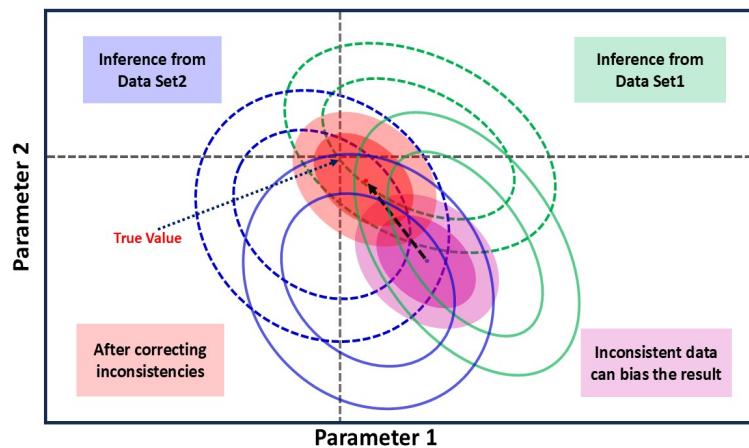


Figure 1: Illustration of how parameter inference from two datasets which are biased can cause precise but an inaccurate inference. The dashed ellipses (green and blue) represent unbiased, independent constraints derived separately from Data Set 1 and Data Set 2, respectively. The solid ellipses (green and blue) indicate the same parameters measured in the presence of uncorrected systematic inconsistencies, causing shifts away from the true parameter values. The magenta filled ellipse shows the biased combined constraint resulting from naively merging these inconsistent measurements. After identifying and correcting the inconsistencies, the corrected combined inference is represented by the red filled ellipse, which realigns closely with the true parameter values. This schematic highlights the necessity of checking and correcting for inter-dataset inconsistencies prior to performing joint cosmological analyses. The boxes in different color explain different contours shown in the figure.

In this work, we apply this consistency test on the latest DESI DR2 release along with the SNIa dataset (Pantheon+) and found a *redshift-dependent breakdown of the CDDR relation* by these two datasets, which indicates towards any unknown physical or systematic effect that is present in the datasets. Moreover, we find that the observed discrepancy can mimic a redshift evolving dark energy model and can bias the inferred value of the dark energy equation of state. We further explore the inference of the dark energy EoS parameters along with the

Hubble constant and matter density, and find that observed discrepancy in the datasets is strongly degenerate with the cosmological parameters. It is important to reiterate that though the breakdown of CDDR seen in the datasets is a cosmological model-independent statement, its presence can bias the cosmological results as luminosity distance and angular diameter distance will drive towards a values away from the true cosmological parameters.

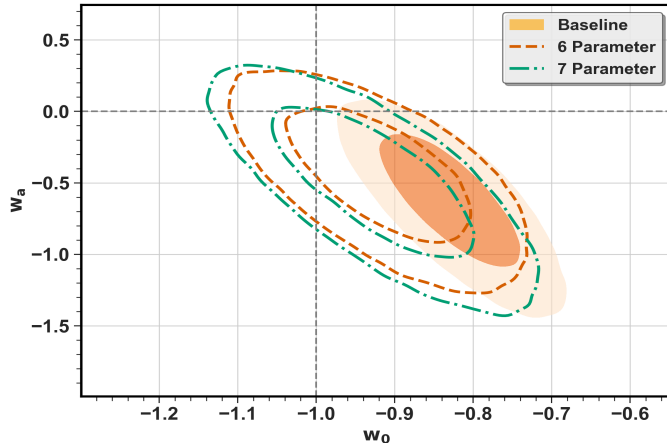


Figure 2: Contours in the dark energy equation of state (EoS) parameters denoted by (w_0, w_a) plane for three analyses: the Baseline fit (without correcting from mismatch in CDDR) (filled orange) constraining $\{H_0, \Omega_m, w_0, w_a\}$; the 6-parameter fit (dashed orange) adding (d_0, d_1) ; and the 7-parameter fit (dash-dot green) further including d_2 (More details are given in Sec. 3). Allowing for distance duality deviations broadens the parameter space and shifts the best-fit region toward the Λ CDM reference point $(w_0 = -1, w_a = 0)$ in agreement with previous cosmological results, highlighting the importance of consistency checks between distance indicators before combining datasets for cosmological inference.

In Figure 2 we show the joint marginalized posteriors on (w_0, w_a) , adopting a Planck 2018 prior on Ω_m [11]. The baseline four-parameter fit (filled orange) yields $(w_0, w_a) \approx (-0.83, -0.62)$. Allowing for CDDR violations by adding two parameters (d_0, d_1) (six-parameter case; dashed orange) broadens the contours and shifts the peak to $(w_0, w_a) \approx (-0.92, -0.44)$. Introducing a third term (d_2) (seven-parameter case; dash-dot green) moves the best-fit even closer to Λ CDM, $(w_0, w_a) \approx (-0.92, -0.49)$. The full numerical results are listed in Table 1. This progression toward $(-1, 0)$ highlights how mild departures from the standard CDDR relation in the data can substantially alter dark energy constraints, and underscores the importance of consistency checks between Pantheon+ and DESI BAO before combining them. With these corrections in place, the DESI+Pantheon inference becomes fully consistent with a cosmological constant.

This paper is organized as follows. In Section 2, we describe the distance duality test used in our study to examine the consistency between various observational datasets. Section 3 focuses on the Pantheon+ and DESI BAO data, assessing the mutual consistency of these datasets. In Section 4, we detail the methodology employed to jointly estimate the cosmological parameters relevant to our analysis. Section 5 summarizes the results of this joint analysis, and Section 6 explores their scientific implications. Finally, Section 7 offers a concise summary of our key findings and suggests avenues for future work.

2 A Primer on the CDDR Test

The CDDR is a fundamental prediction that emerges from photon number conservation in any metric theory of gravity, as articulated by Etherington’s reciprocity theorem. Independent of the details of the cosmological model, the CDDR establishes a connection between the luminosity distance, $D_L(z)$, measured using standard candles (such as SNIa), and the angular diameter distance, $D_A(z)$, determined using standard rulers (such as BAO) at a given redshift z . This relation is expressed as

$$D_L(z) = (1 + z)^2 D_A(z). \quad (2.1)$$

When combining distance measurements from different observational probes, it is crucial to validate the CDDR. Each dataset carries its own systematic uncertainties, and if these are not properly accounted for, hidden biases may jeopardize the joint inference of cosmological parameters. For example, intergalactic dust attenuation, evolution in the properties of supernova progenitors, or even exotic physics could lead to deviations in the observed supernova luminosity distances, thus creating an apparent violation of the CDDR. Such discrepancies may either indicate unaccounted-for astrophysical systematic errors or point toward new physics. This CDDR test has also been done with gravitational waves sources with BAO for a model-independent propagation test of General Relativity as demonstrated in [29–32].

To robustly test for these effects, we introduce a phenomenological distance duality coefficient, $\mathcal{D}(z)$, defined by

$$D_A^{\text{obs1}}(z) = \mathcal{D}(z)(1 + z)^{-2} D_L^{\text{obs2}}(z), \quad (2.2)$$

where $D_A^{\text{obs1}}(z)$ is the angular diameter distance inferred from one type of observation and $D_L^{\text{obs2}}(z)$ is the distance determined from another. Under ideal conditions, we expect $\mathcal{D}(z) = 1$ at all redshifts. Any deviation from unity would signal inconsistencies between the distance measurements, discrepancies that need to be carefully addressed when combining datasets to ensure the integrity of joint cosmological parameter estimation. In principle, one could also perform this consistency test using a fiducial cosmological model by comparing one of the observed distances with the model-predicted distance.

3 Data-Driven CDDR Test for supernovae samples and DESI DR2

We combine the Pantheon+ SNIa data with DESI BAO measurements to evaluate whether the calibrated SNIa distances are consistent with the BAO-inferred distance scale. The distance duality coefficient is defined as

$$D_A^{\text{DESI}}(z) = \mathcal{D}(z)(1 + z)^{-2} D_L^{\text{SNIa}}(z), \quad (3.1)$$

where $D_A^{\text{DESI}}(z)$ is the distance derived from DESI BAO measurements using the CMB-calibrated sound horizon $r_d = 147.09$ Mpc[11], and $D_L^{\text{SNIa}}(z)$ is the distance directly inferred from the SNIa data. We can define a quantity $D_L^{\text{DESI}}(z) \equiv (1 + z)^2 D_A^{\text{DESI}}$, where all the quantities on the right hand side of the equation, comes from data.

In our analysis, the Pantheon+ SNIa data are binned in redshift intervals within the redshift bins (0.1-0.4, 0.4-0.6, 0.6-0.8, 0.8-1.1, and 1.1-1.6). Figure 3 shows the SNIa Pantheon+ distance modulus measurements (in red points) alongside the DESI BAO measurements, illustrating the datasets utilized in our analysis. For each bin, we compute the distance ratio

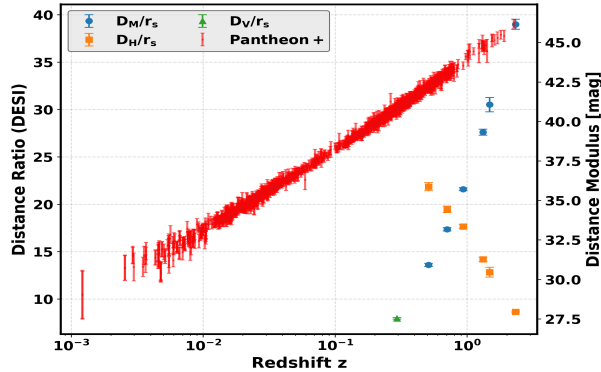


Figure 3: This plot displays two complementary cosmological distance indicators as a function of redshift (plotted on a logarithmic scale). The left y-axis shows the DESI BAO distance ratios D_M/r_s (circles), D_H/r_s (squares), and D_V/r_s (triangles) with corresponding 1σ error bars. The right y-axis presents the Pantheon+ supernova distance modulus used in this analysis.

$(1+z)^2 D_A^{\text{DESI}}(z)/D_L^{\text{SNIa}}(z)$ for each supernova and then determine the median value of the ratio and its corresponding uncertainty. The resulting ratios are plotted in Figure 4. In the absence of any inconsistency one would expect $\mathcal{D}(z) = 1$, but instead we observe a redshift dependent offset $\mathcal{D}(z) > 1$ across all bins. Such a shift could arise from systematic errors in the SNIa calibration or from an incorrect assumption about r_d in the BAO analysis. Redshift-dependent trends might also reflect biases in the BAO fitting procedure or intrinsic evolution of SNIa properties. At present the origin of this discrepancy is unclear, and further work will be required to scrutinize these potential systematics before combining the two datasets for cosmological inference.

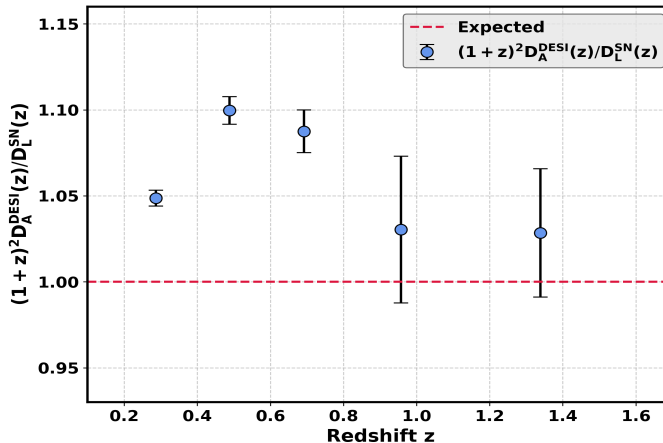


Figure 4: Median ratio of the DESI BAO-inferred luminosity distance to the Pantheon+ SNIa luminosity distance, $\mathcal{D}(z) = (1+z)^2 D_A^{\text{DESI}}(z)/D_L^{\text{SNIa}}(z)$, as a function of redshift. Blue markers with error bars denote the median values of the distance ratio computed in five custom redshift bins (0.1-0.4, 0.4-0.6, 0.6-0.8, 0.8-1.1, and 1.1-1.6), chosen to match the bin choices of the DESI BAO measurements.

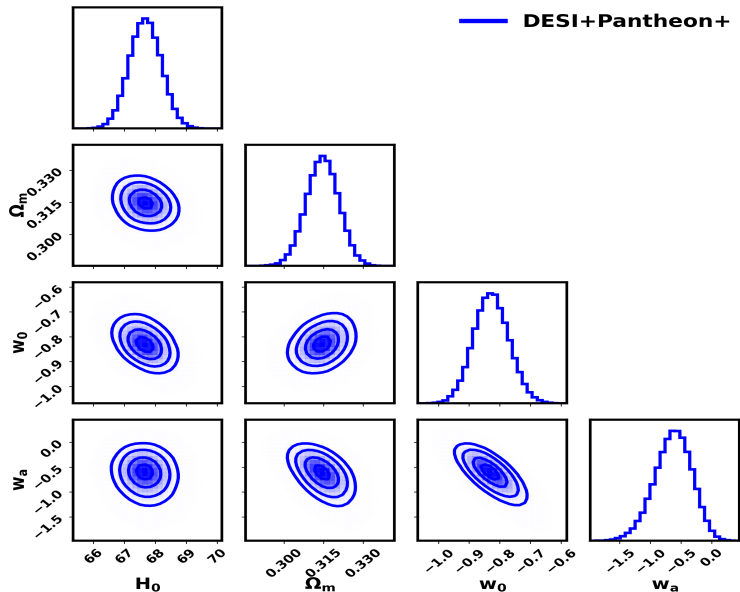


Figure 5: Baseline constraints on $\{H_0, \Omega_m, w_0, w_a\}$ in a flat w_0 - w_a CDM model without including the distance duality parameters. We impose a Gaussian Planck prior on Ω_m with mean 0.315 and standard deviation 0.007, and adopt flat priors on $H_0 \in [60, 80]$, $w_0 \in [-2, 1]$, and $w_a \in [-3, 3]$, together with the requirement $w_0 + w_a < 0$ to restrict to past-light-cone histories.

4 Methodology for Joint Analysis of SNIa and BAO Data

We base our analysis on datasets of SNIa, Pantheon with the measurements from BAO and CMB. In our analysis the comoving sound horizon is fixed to $r_d = 147.09$ Mpc (from Planck [11]), and we adopt the BAO likelihood as implemented in the `cobaya` [33] framework, where it is modeled by a multivariate Gaussian in the compressed parameters with their corresponding covariance matrices. The Pantheon+ Type supernova sample provides distance moduli for 1701 SNIa over the range $0.001 < z < 2.26$ along with the DESI DR11 BAO measurements, which yield compressed distance observables (e.g., $D_M(z)/r_d$, $D_A(z)/r_d$, and $H(z)r_d$) derived from multiple tracers showed in Figure 3.

4.1 Baseline Inference without the Distance Duality Coefficient in the likelihood

In the *baseline model*, we assume that the SNIa luminosity distances conform to a flat $w_0 w_a$ CDM cosmology without any redshift-dependent modification. Concretely, the theoretical SNIa distance modulus is computed as

$$\mu_{\text{th}}(z) = 5 \log_{10} \left[\frac{D_L^{\text{fid}}(z)}{10 \text{ pc}} \right], \quad (4.1)$$

where the fiducial luminosity distance $D_L^{\text{fid}}(z)$ is evaluated using a w_0 - w_a CDM cosmology with the following four parameters $\{H_0, \Omega_m, w_0, w_a\}$. The corresponding SNIa Pantheon+ likelihood takes the form

$$-2 \ln \mathcal{L}_{\text{SNIa}} = \sum_{i,j} \left[\mu_{\text{obs}}(z_i) - \mu_{\text{fid}}(z_i) \right] C_{ij}^{-1} \left[\mu_{\text{obs}}(z_j) - \mu_{\text{fid}}(z_j) \right], \quad (4.2)$$

where $\mu_{\text{obs}}(z_i)$ denotes the observed distance modulus and C_{ij} is the full covariance matrix (including both statistical and systematic uncertainties).

The DESI BAO likelihood is implemented within the `cobaya` framework using CAMB [34] to compute the theoretical BAO observables. It computes the theoretical values for each BAO observable (i.e., D_M/r_s , D_H/r_s , and D_V/r_s) and then compares them to the observed BAO data using the inverse covariance matrix. The corresponding log-likelihood, $-2 \ln \mathcal{L}_{\text{BAO}}$, is therefore given by

$$-2 \ln \mathcal{L}_{\text{BAO}} = \sum_{i,j} \left[\mathcal{D}_{\text{obs}}(z_i) - \mathcal{D}_{\text{th}}(z_i) \right] (C_{\text{BAO}}^{-1})_{ij} \left[\mathcal{D}_{\text{obs}}(z_j) - \mathcal{D}_{\text{th}}(z_j) \right], \quad (4.3)$$

where the theoretical predictions $\mathcal{D}_{\text{th}}(z)$ are a function of $\{H_0, \Omega_m, w_0, w_a\}$ through the background evolution computed by CAMB. The joint likelihood is then constructed by combining the SNIa and BAO likelihoods,

$$\ln \mathcal{L}_{\text{joint}} = \ln \mathcal{L}_{\text{SNIa}} + \ln \mathcal{L}_{\text{BAO}}, \quad (4.4)$$

which is used to constrain the parameter set $\{H_0, \Omega_m, w_0, w_a\}$.

4.2 Extended Inference with a Distance Duality Coefficient

The distance duality coefficient exhibits a redshift-dependent variation and consistently deviates from unity as illustrated in Figure 4. To probe the effect of this variation on the cosmological inference, we incorporate the distance duality coefficient $\mathcal{D}(z)$ into the SNIa likelihood. The inclusion of $\mathcal{D}(z)$ in the likelihood provides a flexible framework for investigating the degeneracy between the distance calibration and the underlying cosmological parameters. In particular any systematic variation in $\mathcal{D}(z)$ can be partially degenerate with shifts in parameters such as H_0 or the dark energy equation of state parameters (w_0, w_a). This structure allows us to diagnose how much of the apparent tension between the SNIa and BAO measurements could be attributed to a breakdown in the standard distance duality relation. Specifically, we define the modified theoretical luminosity distance as

$$D_L^{\text{mod}}(z) \equiv \mathcal{D}(z) D_L^{\text{fid}}(z). \quad (4.5)$$

Accordingly, the modified theoretical SNIa distance modulus becomes

$$\mu_{\text{mod}}(z) = \mu_{\text{fid}}(z) + 5 \log_{10}[\mathcal{D}(z)]. \quad (4.6)$$

This modification leads to the following form for the SNIa likelihood:

$$-2 \ln \mathcal{L}_{\text{SNIa}}^{\text{Modified}} = \sum_{i,j} \left[\mu_{\text{obs}}(z_i) - \mu_{\text{fid}}(z_i) - 5 \log_{10}(\mathcal{D}(z_i)) \right] C_{ij}^{-1} \left[\mu_{\text{obs}}(z_j) - \mu_{\text{fid}}(z_j) - 5 \log_{10}(\mathcal{D}(z_j)) \right]. \quad (4.7)$$

Since $\mathcal{D}(z)$ modifies only the SNIa distances, the BAO likelihood remains unchanged. We thus construct the modified joint likelihood as the product of the SNIa modified and BAO likelihoods,

$$\mathcal{L}_{\text{joint}}^{\text{Modified}} = \mathcal{L}_{\text{SNIa}}^{\text{Modified}} \times \mathcal{L}_{\text{BAO}}. \quad (4.8)$$

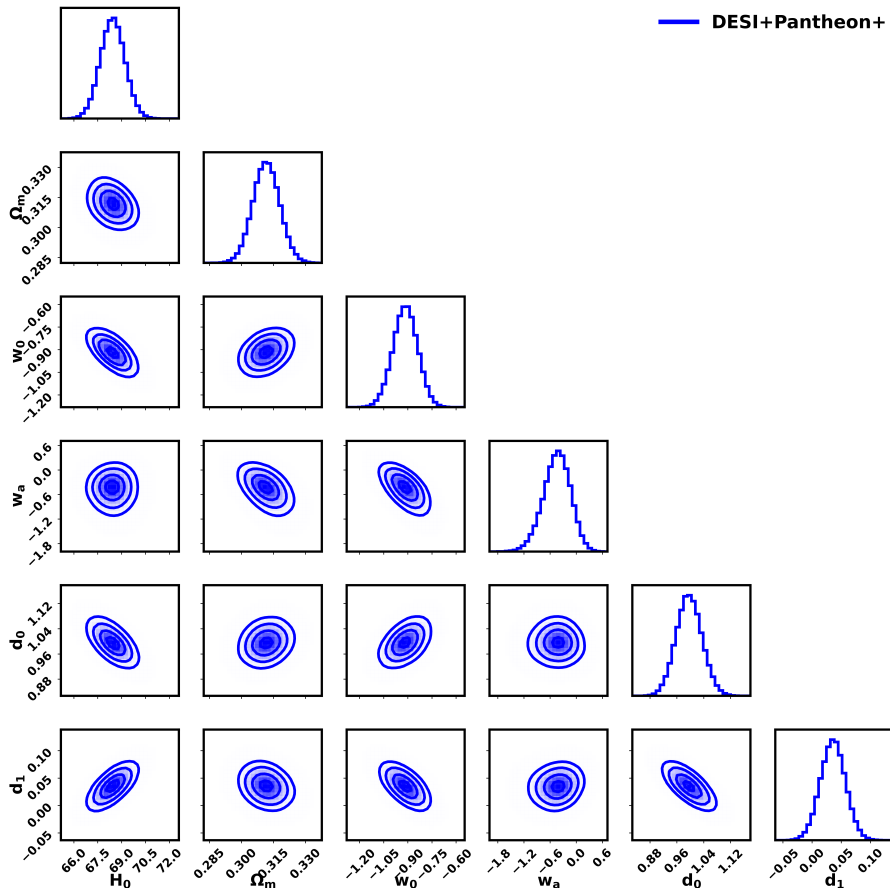


Figure 6: Joint six-parameter posterior constraints on the parameter set $\{H_0, \Omega_m, w_0, w_a, d_0, d_1\}$ in a flat w_0 - w_a CDM model including distance-duality coefficients. We impose a Gaussian Planck prior on Ω_m (mean = 0.315, $\sigma = 0.007$), flat priors on $H_0 \in [60, 80]$, $w_0 \in [-2, 1]$ and $w_a \in [-3, 3]$ with the requirement $w_0 + w_a < 0$, and flat priors on the distance-duality coefficients $d_0 \in [-1, 2]$ and $d_1 \in [-1, 1]$.

Using this joint modified likelihood, we simultaneously fit the cosmological parameters $\{H_0, \Omega_m, w_0, w_a\}$ together with the distance-duality scaling $\mathcal{D}(z)$. We consider two parameterizations of $\mathcal{D}(z)$:

$$\mathcal{D}(z) = d_0 + d_1(1+z), \quad (4.9)$$

$$\mathcal{D}(z) = d_0 + d_1(1+z) + d_2(1+z)^2. \quad (4.10)$$

In the standard distance-duality scenario, one has $d_0 = 1$ and $d_1 = d_2 = 0$, so that $\mathcal{D}(z) = 1$ at all redshifts. We therefore perform:

- a six-parameter analysis $\{H_0, \Omega_m, w_0, w_a, d_0, d_1\}$ using Eq. (4.9), and
- a seven-parameter analysis $\{H_0, \Omega_m, w_0, w_a, d_0, d_1, d_2\}$ using Eq. (4.10),

employing the combined DESI DR2 and Pantheon+ dataset.

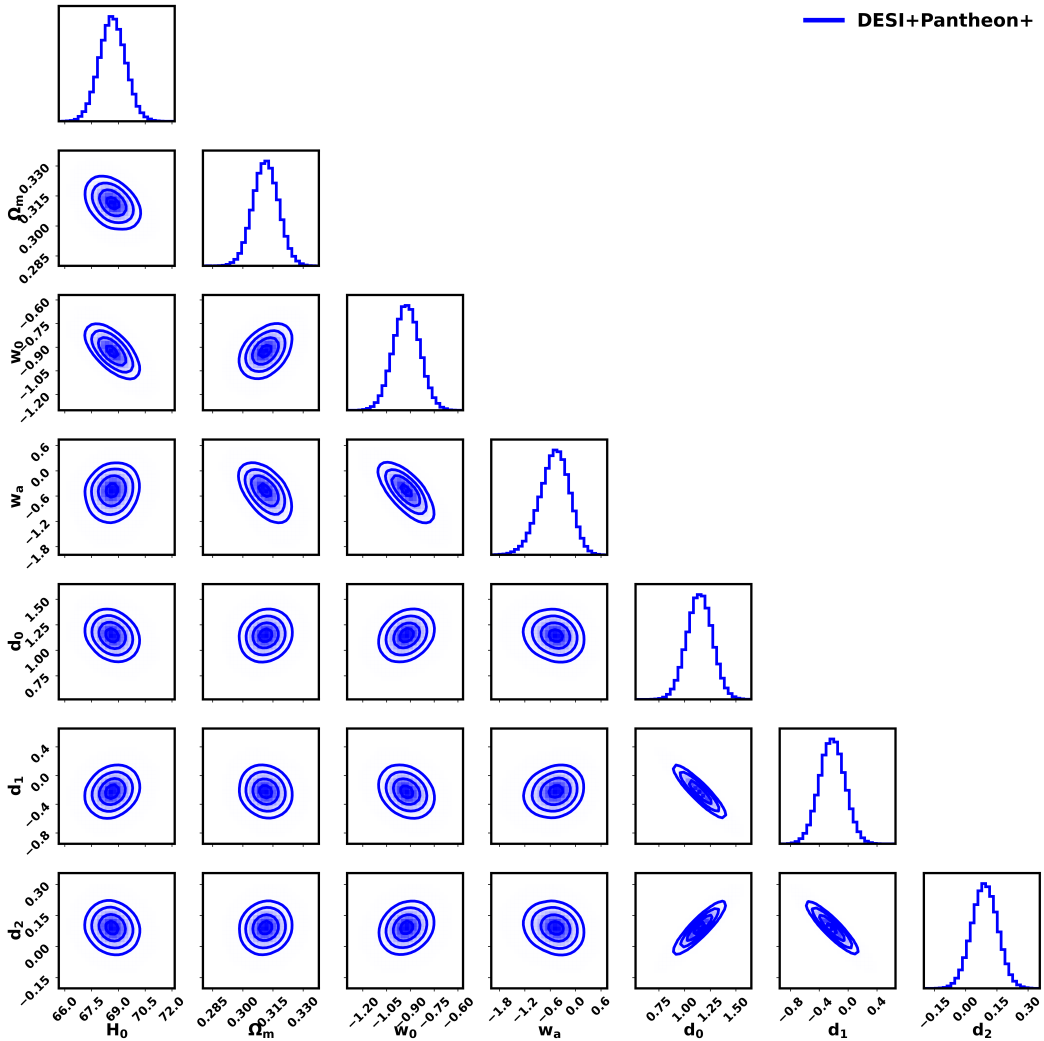


Figure 7: Joint seven-parameter posterior constraints on the parameter set $\{H_0, \Omega_m, w_0, w_a, d_0, d_1, d_2\}$ in a flat w_0 - w_a CDM model including distance duality coefficients. We impose a Gaussian Planck prior on Ω_m (mean = 0.315, $\sigma = 0.007$), flat priors on $H_0 \in [60, 80]$, $w_0 \in [-2, 1]$ and $w_a \in [-3, 3]$ with the requirement $w_0 + w_a < 0$, and flat priors on the distance duality coefficients $d_0 \in [-1, 2]$, $d_1 \in [-1, 1]$ and $d_2 \in [-1, 1]$.

5 Results

5.1 Baseline case: No inclusion of distance-duality coefficient in the likelihood

In Figure 5, we present the posterior distributions for the baseline model obtained by combining the standard Pantheon+ SNIa and DESI BAO likelihoods within a fully Bayesian framework, adopting a Gaussian Planck prior on Ω_m (mean 0.315, $\sigma = 0.007$) and flat priors $H_0 \in [60, 80]$, $w_0 \in [-2, 1]$, and $w_a \in [-3, 3]$ subject to $w_0 + w_a < 0$. Notably, whereas the SNIa data tend to pull the Hubble constant H_0 toward higher values, the BAO measurements favor slightly lower values, resulting in dark-energy parameters that depart from the canonical $(-1, 0)$. In particular, w_0 shifts mildly away from -1 and w_a indicates a slight evolution in

the dark-energy equation of state.

5.2 Extended case: Inclusion of distance-duality coefficient in the likelihood

Figures 6 and 7 display the joint six- and seven-parameter posterior distributions, respectively, obtained from a fully Bayesian analysis combining DESI DR2 and Pantheon+ likelihoods with the modified SNIa model. We impose:

- A Gaussian Planck prior on Ω_m (mean 0.315, $\sigma = 0.007$),
- Flat priors $H_0 \in [60, 80]$, $w_0 \in [-2, 1]$, $w_a \in [-3, 3]$ with $w_0 + w_a < 0$ ¹,
- Flat priors on the distance-duality coefficients $d_0 \in [-1, 2]$, $d_1 \in [-1, 1]$, and (for the seven-parameter case) $d_2 \in [-1, 1]$.

In the six-parameter analysis (Figure 6), introducing d_0 and d_1 broadens the w_0 - w_a contours relative to the baseline and shifts their peak closer to the Λ CDM point ($w_0 = -1$, $w_a = 0$). The overall normalization d_0 remains anchored near unity, while the linear evolution term d_1 shows only a mild redshift dependence. In the seven-parameter analysis (Figure 7), adding the quadratic coefficient d_2 further relaxes the dark-energy constraints, introducing degeneracies among $\{d_0, d_1, d_2\}$. The quadratic term d_2 itself mildly deviates from zero, and d_0 and d_1 exhibit trends similar to the six-parameter case.

An important point to notice from Figures 6 and 7 that there exists strong correlations between the cosmological parameters and the distance-duality parameters (d_0, d_1, d_2). Due to the existence of these correlation, the cosmological parameters can be driven towards an incorrect value, if there exists non-zero contribution from d_0, d_1, d_2 . As a result joint-estimation of the cosmological parameters along with the distance-duality coefficients can reveal possible systematic and can mitigate its influence on the cosmological parameters.

5.3 Summary of all the cases

In this section, we present quantitative results obtained from the combined DESI DR2 and SNIa Pantheon+ datasets under three different modeling assumptions, each progressively introducing additional freedom related to the distance-duality relation. Specifically, we first analyze the baseline w_0 - w_a CDM model (varying only the four cosmological parameters $\{H_0, \Omega_m, w_0, w_a\}$), then extend the analysis to include two distance-duality coefficients (d_0, d_1), and finally further extend to a seven-parameter scenario that incorporates an additional quadratic term d_2 . These incremental extensions enable us to systematically assess how relaxing the standard assumption of distance duality impacts cosmological parameter inference. The full results for all parameters in each model variant are summarized in Table 1.

In Figure 2, we present the joint marginalized posterior distributions in the (w_0, w_a) plane, derived using the combined DESI DR2 and Pantheon+ datasets under different modeling assumptions about the distance-duality relation. The baseline analysis (filled orange contours) constrains the parameters $\{H_0, \Omega_m, w_0, w_a\}$ without any corrections to distance duality. Here, the posterior is relatively tight and centered near $(w_0, w_a) = (-0.83, -0.62)$, slightly offset from the canonical Λ CDM point $(-1, 0)$, agreeing with the Pantheon+ SNIa and DESI BAO results [10].

¹This is imposed to obtain the results to be consistent with DESI DR2 [10]

Summary of the Constraints on the cosmological parameters and $\mathcal{D}(z)$ parameters.							
Model	H_0	Ω_m	w_0	w_a	d_0	d_1	d_2
w_0 - w_a CDM	$67.07^{+0.51}_{-0.51}$	$0.31^{+0.01}_{-0.01}$	$-0.83^{+0.06}_{-0.06}$	$-0.62^{+0.29}_{-0.32}$	-	-	-
w_0 - w_a CDM + (d_0, d_1)	$68.43^{+0.76}_{-0.76}$	$0.31^{+0.01}_{-0.01}$	$-0.92^{+0.08}_{-0.08}$	$-0.44^{+0.29}_{-0.32}$	$1.00^{+0.04}_{-0.04}$	$0.04^{+0.02}_{-0.02}$	-
w_0 - w_a CDM + (d_0, d_1, d_2)	$68.66^{+0.73}_{-0.72}$	$0.31^{+0.01}_{-0.01}$	$-0.92^{+0.08}_{-0.08}$	$-0.49^{+0.33}_{-0.36}$	$1.15^{+0.12}_{-0.12}$	$-0.22^{+0.18}_{-0.17}$	$0.09^{+0.06}_{-0.06}$

Table 1: Summary of the measured values for the Hubble constant H_0 , matter density Ω_m , the dark energy equation of state parameters (w_0, w_a), and the distance duality coefficients (d_0, d_1, d_2). Results are shown for three successive model variants: the baseline w_0 - w_a CDM model without any distance duality parameters, the extension including two coefficients (d_0, d_1), and the full extension with all three coefficients (d_0, d_1, d_2).

However, when we extend our analysis to allow for deviations in the CDDR by introducing additional parameters (d_0, d_1) (the six-parameter scenario, dashed orange contours), we observe a clear shift in the central value of the w_0 and w_a parameters toward $(w_0, w_a) = (-0.92, -0.44)$, closer to the Λ CDM prediction and also broadening of the error-bar. This indicates that the observed tension between datasets may partially (or completely) driven the signature of evolution of the dark energy EoS. Furthermore, the introduction of an additional quadratic parameter d_2 (the seven-parameter scenario, green dash-dot contours) broadens the constraints even further, slightly altering the posterior peak to approximately $(w_0, w_a) = (-0.92, -0.49)$. Although the quadratic coefficient d_2 itself remains consistent with zero, its inclusion significantly relaxes the dark-energy constraints and highlights additional degeneracies among the parameters, as shown by the increasingly elongated shape of the contours.

These results clearly demonstrate that inconsistent datasets can substantially affect the inferred dark-energy EoS parameters. In particular, the additional freedom allowed by the CDDR consistency reduces the apparent mild tension between Pantheon+ and DESI BAO data and significantly weakens the claim of evolving dark energy EoS. This work demonstrates the signatures of possible inconsistencies in the datasets and indicate that the current DESI DR2 with Pantheon+ results are likely to be impacted by this. This makes their analyses precise (due to combining large volume of data), but inaccurate in the inference of cosmological parameters. In future, CDDR tests proposed here, will be important to carry out on different datasets to test for consistency between different datasets.

6 Discussion on the scientific implication of our findings

A rigorous consistency test between independent cosmological probes is essential for precise and reliable parameter estimation. When combining datasets each affected by its own systematic uncertainties hidden biases can lead to erroneous joint inferences. For example, unrecognized redshift-dependent systematics in SNIa may distort the inferred luminosity distances, potentially yielding a spurious evolution in the dark energy equation of state. It is equally important to consider that BAO measurements are not immune to systematic errors. DESI BAO data, while robust and internally consistent, can be subject to uncertainties in the determination of the comoving sound horizon r_d and residual systematics in the large-scale clustering analysis. These BAO specific uncertainties can further complicate the compari-

son of distance scales derived from different probes. Therefore, verifying the consistency of distance measures from SNIa and BAO is crucial to avoid biases in the joint cosmological inference. Such consistency tests ensure that the combined constraints reliably reflect the true underlying cosmology, rather than being driven by mismatched systematics inherent in any single dataset. This approach is especially important for future analyses that will merge supernova data with large-scale structure measurements, where the sensitivity to even subtle systematic effects will be significantly enhanced. The introduction of a redshift-dependent distance-duality coefficient $\mathcal{D}(z)$ has proven effective in capturing the possible systematics in the SNIa Pantheon+ dataset and the DESI BAO dataset. We interpret this result in two possible ways, each with important implications:

Astrophysical Systematics in SNIa: The need for $\mathcal{D}(z) \neq 1$ may indicate residual systematics in SNIa standardization or calibration. Pantheon+ is a meticulously standardized sample, yet combining dozens of surveys and applying empirical bias corrections could leave small redshift-dependent offsets. In our analysis, $\mathcal{D}(z)$ effectively models a smooth version of such an offset.

Evolution of SNIa properties: If the average properties of SNIa progenitors (e.g. metallicity, delay time) shift with redshift, the standardized luminosity might slowly drift. For instance, higher- z SNIa occur in lower-metallicity environments on average, which could make them slightly fainter. Such effects are expected to be small, but a few hundredths of a magnitude over $\Delta z \sim 1$ is not implausible [35–39].

Unaccounted dust contamination: While the SNIa light-curve fits correct for color, a form of extinction that is wavelength-gray (or a circumgalactic/intergalactic component not fully captured by color corrections) could dim distant SNIa more than nearby ones. This could manifest as an $\mathcal{D}(z) > 1$ [40–44].

Calibration drift: Combining many SNIa surveys (some at low z , some at high z) relies on calibrations which are associated with systematic uncertainties [45, 46]. SNIa dataset has gone through several rigorous validation, more recently including JWST observations [47]. However, presence of any non-zero systematic calibration error between low- z and high- z samples could appear as a distance modulus shift.

Selection biases: Malmquist bias (brightness selection effects) and survey strategy differences can cause subtle redshift-dependent biases in the observed SNIa population. The Pantheon+ analysis includes corrections for selection bias as a function of redshift; however, if these corrections are slightly mis-estimated, an residual trend in Hubble residuals vs. z might remain. If indeed $\mathcal{D}(z)$ is attributable to SNIa systematics, then our results underscore the importance of continually refining SNIa analyses [48–50]. Future SNIa samples from LSST (Rubin Observatory [51]) and JWST [52] can probe higher redshifts with improved calibration, allowing direct tests of whether SNIa brightness evolves.

Systematic Uncertainties in BAO and CMB: BAO and CMB measurements are widely regarded as robust anchors of the cosmic distance scale, yet they are not immune to systematic errors. For BAO, uncertainties can arise from inaccuracies in BAO modeling which may slightly shift the measured distance observables, such as $D_M(z)/r_d$ and $H(z)r_d$ [53–55]. Additionally, the determination of the sound horizon r_d from the CMB involves assumptions about the physics of the early universe such as the baryon density and recombination history which, if are calculated incorrectly, can introduce unaccounted residual uncertainties. For CMB observations, systematic issues may stem from instrumental calibration, beam uncertainties, and the subtraction of foreground contaminants. Although these systematics are typically sub-dominant compared to the high statistical precision of modern CMB experi-

ments, they nonetheless contribute to the overall error budget in the inferred cosmological parameters [56–58].

Exotic Physics Affecting Distance Measures: Alternatively, $\mathcal{D}(z)$ may indicate new physics beyond the standard model. One possibility is a violation of the CDDR, which states that $D_L = (1 + z)^2 D_A$ under photon number conservation. Physical mechanisms that could lead to a CDDR violation include photon mixing with axion-like particles or absorption by an opaque dark sector. In such scenarios, a fraction of photons could oscillate into axions over cosmological distances, resulting in an energy-independent dimming of SNIa. Although current CMB and X-ray constraints limit these effects, a percent-level reduction in flux remains plausible. In this context, a nonzero d_1 may hint at a light scalar field coupling to photons, with an interaction probability that accumulates with $(1 + z)$ [59–64].

A key difference between systematic errors and a new physical effect is that the latter should uniformly affect all luminous sources, while SNIa-specific systematics would not impact BAO or CMB observations. Since BAO and CMB data agree while SNIa do not, our results favor a scenario in which correcting for the SNIa-specific $\mathcal{D}(z)$ restores consistency with vanilla Λ CDM. This outcome suggests that the discrepancies are more likely due to unaccounted astrophysical systematics rather than a universal new physics effect, although the possibility of a subtle new interaction cannot be entirely ruled out.

7 Conclusion

This analysis explores the consistency test based on the CDDR of SNIa and BAO datasets used for the inference of the low redshift expansion history of the Universe by the DESI collaboration. We find that SNIa datasets and BAO datasets fails to match the fundamental CDDR and depict a statistically significant bias across most of the low redshift range. The failure of this consistency test hint towards possible unaccounted systematics present in these datasets and hence refutes the robustness of the cosmological inference obtained using DESI and SNIa in combination with the CMB information.

Our analysis points out that there exists a strong correlation between the cosmological parameters and the parameters which can capture the deviation from CDDR. As a result, presence of any effect which violates CDDR can bias the inference of cosmological parameters. On taking into account the CDDR in terms of a redshift-dependent phenomenological model to fit the data, we find that both the dark energy EoS parameters w_0 and w_a show a strong degeneracy with the parameters capturing the CDDR deviation. Moreover, the posterior of the dark energy EoS parameters shifts towards the value of $w_0 = -1$ and $w_a = 0$ which is consistent with the dark energy model as cosmological constant. This implies a consistent inference of the cosmological parameters is possible when the deviations from CDDR are marginalized over.

In summary, the recent claim of evolving dark energy EoS by the DESI collaboration using the low redshift cosmological probe is subject to unaccounted systematic (astrophysical or non-astrophysical) effects. Such contamination is likely causing an inaccurate inference of the cosmological parameters from these datasets. Combining independent datasets that are impacted by systematic can cause a precise but inaccurate inference of cosmological parameters. Our study provides a clue towards this direction and in the future more elaborate study will be required to explore the reason for this effect. Also, future cosmological analysis using different independent datasets must perform CDDR consistency tests, to confirm that possible contamination from systematic effect in either datasets is not driving the cosmological

results. In the future with the availability of multi-messenger cosmological datasets by the addition of gravitational wave source catalog of bright standard sirens, both accurate and precision measurement of the dark energy will be feasible [25].

Author’s note: When this study was under preparation, papers [65–67] by other authors also appeared on arXiv that indicates a similar issue with the DESI and SNIa datasets.

Acknowledgements

This work is part of the `<data|theory>` Universe-Lab, supported by TIFR and the Department of Atomic Energy, Government of India. The authors thank the computing cluster of the `<data|theory>` Universe-Lab for providing computing resources. We acknowledge the use of publicly available data from the Pantheon+ supernova sample [16] and the DESI BAO measurements [10], as well as several software packages that significantly facilitated this analysis: Astropy [68], Pandas [69], NumPy [70], Seaborn [71], SciPy [72], emcee [73], pygtdc [74], corner [75], and Matplotlib [76].

References

- [1] David H. Weinberg, Michael J. Mortonson, Daniel J. Eisenstein, Christopher Hirata, Adam G. Riess, and Eduardo Rozo. Observational probes of cosmic acceleration. *Phys. Rep.*, 530(2):87–255, September 2013.
- [2] Ofer Lahav and Andrew R. Liddle. The Cosmological Parameters (2023). 3 2024.
- [3] Denitsa Staicova. Modern Bayesian Sampling Methods for Cosmological Inference: A Comparative Study. *Universe*, 11(2):68, 2025.
- [4] José Luis Bernal and John A. Peacock. Conservative cosmology: combining data with allowance for unknown systematics. *JCAP*, 07:002, 2018.
- [5] Davide Piras, Alicja Polanska, Alessio Spurio Mancini, Matthew A. Price, and Jason D. McEwen. The future of cosmological likelihood-based inference: accelerated high-dimensional parameter estimation and model comparison. 5 2024.
- [6] Charles L. Steinhardt, Preston Phillips, and Radoslaw Wojtak. Dark Energy Constraints and Joint Cosmological Inference from Mutually Inconsistent Observations. 4 2025.
- [7] Elcio Abdalla et al. Cosmology intertwined: A review of the particle physics, astrophysics, and cosmology associated with the cosmological tensions and anomalies. *JHEAp*, 34:49–211, 2022.
- [8] Anthony Carr, Tamara M. Davis, Dan Scolnic, Daniel Scolnic, Khaled Said, Dillon Brout, Erik R. Peterson, and Richard Kessler. The Pantheon+ analysis: Improving the redshifts and peculiar velocities of Type Ia supernovae used in cosmological analyses. *Publ. Astron. Soc. Austral.*, 39:e046, 2022.
- [9] T. M. C. Abbott et al. First Cosmology Results using Type Ia Supernovae from the Dark Energy Survey: Constraints on Cosmological Parameters. *Astrophys. J. Lett.*, 872(2):L30, 2019.
- [10] M. Abdul Karim et al. DESI DR2 Results II: Measurements of Baryon Acoustic Oscillations and Cosmological Constraints. 3 2025.
- [11] N. Aghanim et al. Planck 2018 results. VI. Cosmological parameters. *Astron. Astrophys.*, 641:A6, 2020. [Erratum: *Astron. Astrophys.* 652, C4 (2021)].
- [12] Pablo Lemos and Paul Shah. The Cosmic Microwave Background and H_0 . 7 2023.

- [13] Thibaut Louis et al. The Atacama Cosmology Telescope: DR6 Power Spectra, Likelihoods and Λ CDM Parameters. 3 2025.
- [14] T. M. C. Abbott et al. The Dark Energy Survey Data Release 1. *Astrophys. J. Suppl.*, 239(2):18, 2018.
- [15] Amir Aghamousa et al. The DESI Experiment Part I: Science, Targeting, and Survey Design. 10 2016.
- [16] Dillon Brout et al. The Pantheon+ Analysis: Cosmological Constraints. *Astrophys. J.*, 938(2):110, 2022.
- [17] David Rubin et al. Union Through UNITY: Cosmology with 2,000 SNe Using a Unified Bayesian Framework. 11 2023.
- [18] T. M. C. Abbott et al. The Dark Energy Survey: Cosmology Results with ~ 1500 New High-redshift Type Ia Supernovae Using the Full 5 yr Data Set. *Astrophys. J. Lett.*, 973(1):L14, 2024.
- [19] Michel Chevallier and David Polarski. Accelerating universes with scaling dark matter. *Int. J. Mod. Phys. D*, 10:213–224, 2001.
- [20] Eric V. Linder. Exploring the expansion history of the universe. *Phys. Rev. Lett.*, 90:091301, 2003.
- [21] Roland de Putter and Eric V. Linder. Calibrating Dark Energy. *JCAP*, 10:042, 2008.
- [22] A. G. Adame et al. DESI 2024 III: baryon acoustic oscillations from galaxies and quasars. *JCAP*, 04:012, 2025.
- [23] David Shlivko and Paul J. Steinhardt. Assessing observational constraints on dark energy. *Phys. Lett. B*, 855:138826, 2024.
- [24] William J. Wolf and Pedro G. Ferreira. Underdetermination of dark energy. *Phys. Rev. D*, 108:103519, Nov 2023.
- [25] Samsuzzaman Afroz and Suvodip Mukherjee. Multi-messenger cosmology: A route to accurate inference of dark energy beyond CPL parametrization from XG detectors. *JCAP*, 03:070, 2025.
- [26] R. F. L. Holanda, J. A. S. Lima, and M. B. Ribeiro. Testing the Distance-Duality Relation with Galaxy Clusters and Type Ia Supernovae. *Astrophys. J. Lett.*, 722:L233–L237, 2010.
- [27] Kai Liao, Zhengxiang Li, Shuo Cao, Marek Biesiada, Xiaogang Zheng, and Zong-Hong Zhu. The Distance Duality Relation From Strong Gravitational Lensing. *Astrophys. J.*, 822(2):74, 2016.
- [28] I. M. H. Etherington. Republication of: LX. On the definition of distance in general relativity. *General Relativity and Gravitation*, 39(7):1055–1067, July 2007.
- [29] Samsuzzaman Afroz and Suvodip Mukherjee. Prospect of precision cosmology and testing general relativity using binary black holes – galaxies cross-correlation. *Mon. Not. Roy. Astron. Soc.*, 534(2):1283–1298, 2024.
- [30] Samsuzzaman Afroz and Suvodip Mukherjee. A model-independent precision test of General Relativity using LISA bright standard sirens. *JCAP*, 10:100, 2024.
- [31] Samsuzzaman Afroz and Suvodip Mukherjee. A model-independent precision test of general relativity using bright standard sirens from ongoing and upcoming detectors. *Mon. Not. Roy. Astron. Soc.*, 530(4):3812–3826, 2024.
- [32] Suvodip Mukherjee, Benjamin D. Wandelt, and Joseph Silk. Testing the general theory of relativity using gravitational wave propagation from dark standard sirens. *Mon. Not. Roy. Astron. Soc.*, 502(1):1136–1144, 2021.

- [33] Jesús Torrado and Antony Lewis. Cobaya: Bayesian analysis in cosmology. Astrophysics Source Code Library, record ascl:1910.019, October 2019.
- [34] Antony Lewis, Anthony Challinor, and Anthony Lasenby. Efficient computation of CMB anisotropies in closed FRW models. *Astrophys. J.*, 538:473–476, 2000.
- [35] E. Bravo, I. Domínguez, C. Badenes, L. Piersanti, and O. Straniero. Metallicity as a Source of Dispersion in the SNIa Bolometric Light Curve Luminosity-Width Relationship. *ApJ*, 711(2):L66–L70, March 2010.
- [36] E. Bravo and C. Badenes. Is the metallicity of their host galaxies a good measure of the metallicity of Type Ia supernovae? *MNRAS*, 414(2):1592–1606, June 2011.
- [37] Adam G Riess and Mario Livio. The first type ia supernovae: an empirical approach to taming evolutionary effects in dark energy surveys from sne ia at $z > 2$. *Astrophys. J.*, 648:884–889, 2006.
- [38] Nino Panagia, Massimo Della Valle, and Filippo Mannucci. Type Ia Supernova Rates Near and Far. *AIP Conf. Proc.*, 924(1):373–382, 2007.
- [39] David O. Jones et al. The Discovery of the Most Distant Known Type Ia Supernova at Redshift 1.914. *Astrophys. J.*, 768:166, 2013.
- [40] A. R. Robaina and J. Cepa. Redshift-distance relations from type Ia supernova observations. New constraints on grey dust models. *A&A*, 464(2):465–470, March 2007.
- [41] Ariel Goobar, Suhail Dhawan, and Daniel Scolnic. The cosmic transparency measured with Type Ia supernovae: implications for intergalactic dust. *Mon. Not. Roy. Astron. Soc.*, 477(1):L75–L79, 2018.
- [42] Vaclav Vavrycuk. Universe opacity and Type Ia supernova dimming. *Mon. Not. Roy. Astron. Soc.*, 489(1):L63–L68, 2019.
- [43] Linda Ostman and Edvard Mortsell. Limiting the dimming of distant Type Ia supernovae. *JCAP*, 02:005, 2005.
- [44] Rupert A. C. Croft, Romeel Dave, Lars Hernquist, and Neal Katz. Simulating the effects of intergalactic grey dust. *Astrophys. J. Lett.*, 534:L123, 2000.
- [45] Dillon Brout et al. The Pantheon+ Analysis: SuperCal-fragilistic Cross Calibration, Retrained SALT2 Light-curve Model, and Calibration Systematic Uncertainty. *Astrophys. J.*, 938(2):111, 2022.
- [46] Sasha R. Brownsberger, Dillon Brout, Daniel Scolnic, Christopher W. Stubbs, and Adam G. Riess. Dependence of Cosmological Constraints on Gray Photometric Zero-point Uncertainties of Supernova Surveys. *Astrophys. J.*, 944(2):188, 2023.
- [47] Adam G. Riess et al. JWST Validates HST Distance Measurements: Selection of Supernova Subsample Explains Differences in JWST Estimates of Local H_0 . *Astrophys. J.*, 977(1):120, 2024.
- [48] Benjamin L’Huillier, Arman Shafieloo, Eric V. Linder, and Alex G. Kim. Model Independent Expansion History from Supernovae: Cosmology versus Systematics. *Mon. Not. Roy. Astron. Soc.*, 485(2):2783–2790, 2019.
- [49] M. Toy et al. Reduction of the type Ia supernova host galaxy step in the outer regions of galaxies. *Mon. Not. Roy. Astron. Soc.*, 538(1):181–197, 2025.
- [50] Leandros Perivolaropoulos and Foteini Skara. On the homogeneity of SnIa absolute magnitude in the Pantheon+ sample. *Mon. Not. Roy. Astron. Soc.*, 520(4):5110–5125, 2023.
- [51] LSST Science Collaboration. LSST Science Book, Version 2.0. *arXiv e-prints*, page arXiv:0912.0201, December 2009.

- [52] Jonathan P. Gardner, John C. Mather, Mark Clampin, Rene Doyon, Matthew A. Greenhouse, Heidi B. Hammel, John B. Hutchings, Peter Jakobsen, Simon J. Lilly, Knox S. Long, Jonathan I. Lunine, Mark J. McCaughrean, Matt Mountain, John Nella, George H. Rieke, Marcia J. Rieke, Hans-Walter Rix, Eric P. Smith, George Sonneborn, Massimo Stiavelli, H. S. Stockman, Rogier A. Windhorst, and Gillian S. Wright. The James Webb Space Telescope. *Space Sci. Rev.*, 123(4):485–606, April 2006.
- [53] Zhejie Ding, Hee-Jong Seo, Zvonimir Vlah, Yu Feng, Marcel Schmittfull, and Florian Beutler. Theoretical Systematics of Future Baryon Acoustic Oscillation Surveys. *Mon. Not. Roy. Astron. Soc.*, 479(1):1021–1054, 2018.
- [54] Francisco Prada, Claudia G. Scóccola, Chia-Hsun Chuang, Gustavo Yepes, Anatoly A. Klypin, Francisco-Shu Kitaura, Stefan Gottlöber, and Cheng Zhao. Hunting down systematics in baryon acoustic oscillations after cosmic high noon. *Mon. Not. Roy. Astron. Soc.*, 458(1):613–623, 2016.
- [55] Takahiro Nishimichi, Eugenio Noda, Marco Peloso, and Massimo Pietroni. BAO Extractor: bias and redshift space effects. *JCAP*, 01:035, 2018.
- [56] Maximilian H. Abitbol, J. C. Hill, and B. R. Johnson. Foreground-Induced Biases in CMB Polarimeter Self-Calibration. *Mon. Not. Roy. Astron. Soc.*, 457(2):1796–1803, 2016.
- [57] P. A. R. Ade et al. Planck 2015 results. III. LFI systematic uncertainties. *Astron. Astrophys.*, 594:A3, 2016.
- [58] Jonathan Aumont, Juan Francisco Macías-Pérez, Alessia Ritacco, Nicolas Ponthieu, and Anna Mangilli. Absolute calibration of the polarisation angle for future CMB B -mode experiments from current and future measurements of the Crab nebula. *Astron. Astrophys.*, 634:A100, 2020.
- [59] Csaba Csaki, Nemanja Kaloper, and John Terning. Dimming supernovae without cosmic acceleration. *Phys. Rev. Lett.*, 88:161302, 2002.
- [60] Bruce A. Bassett. Cosmic acceleration vs axion - photon mixing. *Astrophys. J.*, 607:661–664, 2004.
- [61] Alessandro Mirizzi, Georg G. Raffelt, and Pasquale D. Serpico. Photon-axion conversion in intergalactic magnetic fields and cosmological consequences. *Lect. Notes Phys.*, 741:115–134, 2008.
- [62] R. F. L. Holanda, R. S. Gonçalves, and J. S. Alcaniz. A test for cosmic distance duality. *JCAP*, 06:022, 2012.
- [63] Alessandro Mirizzi, Georg G. Raffelt, and Pasquale D. Serpico. Photon-axion conversion as a mechanism for supernova dimming: Limits from CMB spectral distortion. *Phys. Rev. D*, 72:023501, 2005.
- [64] Anson Hook, Gustavo Marques-Tavares, and Clayton Ristow. Supernova constraints on an axion-photon-dark photon interaction. *JHEP*, 06:167, 2021.
- [65] Elsa M. Teixeira, William Giarè, Natalie B. Hogg, Thomas Montandon, Adèle Poudou, and Vivian Poulin. Implications of distance duality violation for the H_0 tension and evolving dark energy. 4 2025.
- [66] Deng Wang and David Mota. Did DESI DR2 truly reveal dynamical dark energy? 4 2025.
- [67] Marina Cortês and Andrew R Liddle. On DESI’s DR2 exclusion of Λ CDM. *arXiv e-prints*, page arXiv:2504.15336, April 2025.
- [68] Adrian M Price-Whelan, BM Sipőcz, HM Günther, PL Lim, SM Crawford, S Conseil, DL Shupe, MW Craig, N Dencheva, A Ginsburg, et al. The astropy project: building an open-science project and status of the v2. 0 core package. *The Astronomical Journal*, 156(3):123, 2018.

- [69] Wes McKinney et al. pandas: a foundational python library for data analysis and statistics. *Python for high performance and scientific computing*, 14(9):1–9, 2011.
- [70] Charles R Harris, K Jarrod Millman, Stéfan J Van Der Walt, Ralf Gommers, Pauli Virtanen, David Cournapeau, Eric Wieser, Julian Taylor, Sebastian Berg, Nathaniel J Smith, et al. Array programming with numpy. *Nature*, 585(7825):357–362, 2020.
- [71] Ekaba Bisong and Ekaba Bisong. Matplotlib and seaborn. *Building Machine Learning and Deep Learning Models on Google Cloud Platform: A Comprehensive Guide for Beginners*, pages 151–165, 2019.
- [72] Pauli Virtanen, Ralf Gommers, Travis E Oliphant, Evgeni Burovski, David Cournapeau, Warren Weckesser, Pearu Peterson, Stefan van der Walt, Denis Laxalde, Matthew Brett, et al. Scipy/scipy: Scipy 0.19. 0. *Zenodo*, 2020.
- [73] Daniel Foreman-Mackey, David W Hogg, Dustin Lang, and Jonathan Goodman. emcee: the mcmc hammer. *Publications of the Astronomical Society of the Pacific*, 125(925):306, 2013.
- [74] Sebastian Bocquet and Faustin W Carter. pygtc: Parameter covariance plots. *Astrophysics Source Code Library*, pages ascl–1907, 2019.
- [75] Daniel Foreman-Mackey. corner.py: Scatterplot matrices in python. *The Journal of Open Source Software*, 1(2):24, jun 2016.
- [76] J. D. Hunter. Matplotlib: A 2d graphics environment. *Computing in Science & Engineering*, 9(3):90–95, 2007.